

Variable optical attenuator using planar light attenuation scheme based on rotational and translational misalignment

Chengkuo Lee

Received: 13 March 2006 / Accepted: 31 August 2006 / Published online: 12 October 2006
© Springer-Verlag 2006

Abstract In the last decade, extensive developments of microelectromechanical systems based thermal actuator and/or electrothermal actuators have been dedicated to the applications, such as data storage devices, relays and optical switches, etc. In this paper, we demonstrated a novel planar micromechanism comprising a tilted mirror driven by a V-beam electrothermal actuator via a link beam. This electrothermally driven tilted mirror can have static displacement with a motion trace including rotational and translational movement. The rotational and translational misalignment of reflected light spot toward the core of output port fiber will lead to light attenuation. In other words, the attenuation is controlled in terms of the position of tilted mirror depending on driving dc voltage. This new micromechanism has granted us a more efficient way to perform the light attenuation regarding to the other kinds of planar variable optical attenuators. These devices were fabricated by the deep reactive ion etching process and can reach 30-dB attenuation at 7.5 V driving voltage. The polarization dependant loss is less than 0.1 dB within the 30-dB attenuation region. The static and transient characteristics of devices operated at ambient room temperature environment show good repeatability and stability.

1 Introduction

Microelectromechanical systems (MEMS) actuators for planar dynamic motion or static displacement have received consistent attention in research since years ago. The electrothermal actuators have been known as their large displacement and high force output (DeVoe 2002). The V-beam actuator (Gianchandani and Najafi 1996; Que et al. 2001) and U-shaped actuator (Pan and Hsu 1997; Huang and Lee 1999) are the two most cited and characterized electrothermal actuators, while two new sorts of electrothermal actuators, i.e., X-shaped and H-shaped electrothermal actuators, have been reported recently (Lee and Yeh 2005; Lee 2006a). Usage of V-beam actuators for planar displacement, for moving LIGA X-ray mask (Lee and Lee 2004), and bi-stable optical switch (Lee and Wu 2005) has demonstrated the potential of electrothermal actuators for practical applications.

On the other hand, variable optical attenuator (VOA) is commonly adopted as a key component to groom power levels across the WDM spectrum, to minimize the crosstalk and to maintain the desired signal-to-noise ratio. The MEMS VOAs (Ford and Walker 1998; Barber et al. 1998; Marxer et al. 1999) deploy the free space light attenuation technology, and demonstrate their prevalence advantages over other solutions in terms of device features of wavelength independence, and protocol and bit rate independence, etc. Thus MEMS VOAs can reduce incoming light intensity in an analog control manner regardless the difference of wavelength and protocol. The function of controllably attenuating a light beam can be achieved by various methods, among previously reported MEMS VOAs, such as, by partially blocking the beam

C. Lee (✉)
Department of Electrical and Computer Engineering,
National University of Singapore, 4 Engineering Drive 3,
Singapore, Singapore 117576
e-mail: elelc@nus.edu.sg

C. Lee
Institute of Microelectronics, A*STAR,
11 Science Park Road,
Singapore, Singapore 117685

via inserting a beam shutter into the light beam path, i.e., the planar shutter type (Barber et al. 1998; Marxer et al. 1999; Liu et al. 2003; Kim et al. 2004); by changing the position of one or two in-plane movable mirrors relative to input/output fibers, to alter the coupling efficiency of light from/toward the fibers in terms of one reflection or two reflections configurations, respectively, i.e., the planar reflection (Chen et al. 2003a, b; Lee 2005a; Bashir et al. 2004) and retro-reflection types (Chen et al. 2004; Lee 2005b); by using an axial moving elliptical-mirror to modify the focal spot of reflected light beam toward the output fiber (Cai et al. 2005); and by adopting a three-dimensional (3D) tilted mirror to redirect the reflected light beam direction toward the output fiber, where this tilted mirror is placed facing a convergent lens in front of end faces of two parallel fibers in a 3D configuration (Robinson 2000; Costello et al. 2003; Isamoto et al. 2004). All the aforementioned MEMS VOAs were based on electrostatic actuation mechanisms, i.e., the comb drive actuators and the parallel plate actuators.

Recently the V-beam electrothermal actuator has been applied to drive a shutter for a 3D configured MEMS VOA applications (Syms et al. 2004). A micromechanism driven by a set of U-shaped electrothermal actuator to rotate a surface micromachined pop-up mirror is used to steer the planar propagated light reflect toward out-of-plane direction (Lee et al. 2004). Thus the attenuation range is determined by the out-of-plane rotational angle of the pop-up mirror. Moreover, it was reported that MEMS VOA of a planar attenuation scheme has been demonstrated by using two pairs of U-shaped electrothermal actuators linked together to push two shutters on opposite sides to block the light in parallel (Chiou and Lin 2004). H-shaped electrothermal actuators are applied to realize a retro-reflection type MEMS VOA (Lee 2006b) with the advantage of smaller footprint and better mechanical stability. In this paper, a novel micromechanism is proposed to perform planar attenuation by reducing the coupled light intensity. The feasibility study and preliminary testing data are reported.

2 Attenuation mechanism, device design and simulation

Figure 1a shows the schematic drawing of the configuration of reflective tilted mirror and light path in its initial state. Without driving the mirror to tilt, the locations and angles regarding to the input and output fibers are adjusted to reach the optimized coupling

state. As shown in Fig. 1b, when the actuator is in operation, the mirror will be tilted to let the reflected beam deviated from original optimized path of AO to A'F'. In case of considering the attenuation scheme based on rotational effect only, the incoming light spot incidents on A point and redirects toward F point. The angle between the dotted AF line of reflected light path due to rotational effect of mirror and the dotted AO line of original reflected light path at the non-attenuation state is observed as of $2\emptyset$, where the \emptyset represents the mirror rotational angle. Additionally Fig. 1b, c show that one end of mirror is held by a meander spring, where this spring is anchored on substrate and could be bended due to the force from electrothermal actuator. Based on the proposed novel micromechanism, a translational displacement (t) for mirror is generated due to the bending effect of the meander spring. This translational displacement leads the reflected light path further deviating from the AF line to A'F' line. It means the overall attenuation comprising rotational and translational contribution, i.e., including $2\emptyset$ and t . It points out the present micromechanism can provide more efficient attenuation approach than previous technologies. The VOA using tilted mirror based on this micromechanism is reported first time.

The main considerations of designing appropriate V-beam actuators are force output and displacement. Cochran et al. (Cochran et al. 2003; Maloney et al. 2004) have developed a model to derive the maximum force output, denoted as the F_t , from a single V-beam actuator. Assuming thermal conductivity and the coefficient of thermal expansion are temperature independent, the steady state heat equation is:

$$k_s \frac{dT(x)}{dx^2} + J^2 \rho - Sk_a \frac{T(x) - 273}{gh} = 0 \quad (1)$$

Solving Eq. (1) for temperature will derive,

$$T(x) = 273 + \frac{J^2 \rho}{k_p gh} \left[1 - \frac{\cosh(mL/2) - mx}{\cosh(mL/2)} \right] \quad (2)$$

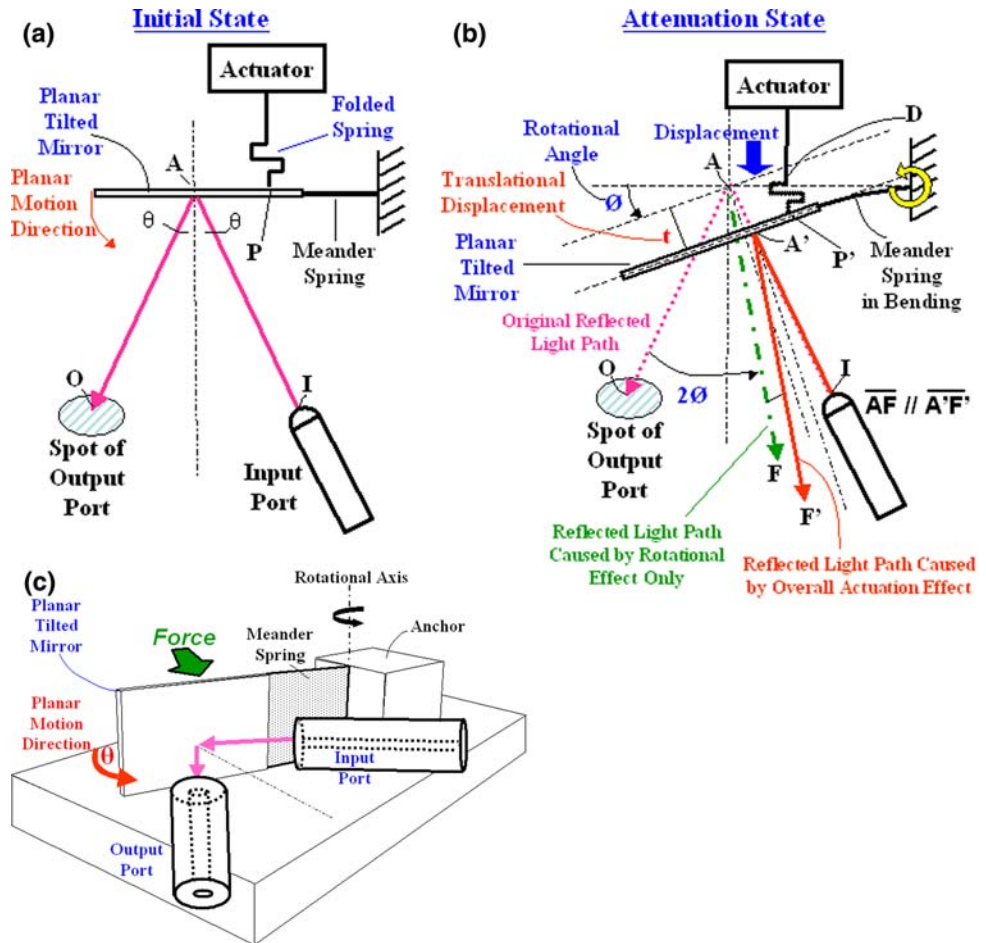
$$m = \frac{Sk_a}{k_s gh} \quad (3)$$

$$S = \frac{h \left[\left(\frac{2g}{h} \right) + 1 \right] + w}{w} \quad (4)$$

$$\frac{F_t}{P} = \frac{4\alpha CE d}{K_s m^2 L^2} \left[1 - \frac{2 \tanh(mL/2)}{mL} \right] \quad (5)$$

$$P = whLJ^2 \rho \quad (6)$$

Fig. 1 Novel planar light attenuation scheme by using a tilted mirror with rotational and translational displacement. **a** Tilted mirror device at its initial state (zero attenuation); **b** Tilted mirror device at its attenuation state. **c** The 3D schematic drawing of VOA using proposed micromechanism



where the P is the electrical power. As shown in Fig. 2a, L , w , h , and d denote V-beam length, width, thickness, and center offset distance, respectively. Besides, the g is defined as the gap between the bottom of V-beam actuator and the substrate, where it is $2\ \mu\text{m}$. The other parameters listed in Table 1 include ρ of the resistivity of silicon, J of the current density, α of the thermal expansion coefficient of silicon, k_a and k_s of the thermal conductivities of the air and silicon; S of the shape parameter which means the ratio of the heat loss from sides and bottom of the V-beam to the heat loss from the bottom of the beam only. In present case, the C is the experimental correlation factor regarding to excessive deflection based on measured data and is set as 1.5, and the up-limit of silicon temperature caused by joule heating is set as 800 K in the center of V-beam actuator, the function of $T(x)$ means the temperature variation of V-beam, x means the position along with the beam.

Thus the generated displacement is given by:

$$u(\theta) = P \left(1 - \frac{2 \tanh\left(m\frac{L}{2}\right)}{mL} \right) \frac{C\alpha L d(\theta)}{4whk_s m^2 (d(\theta)^2 + w^2)} \quad (7)$$

where $u(\theta)$ means the relation between displacement and θ , θ means the tilted angle of V-beam to perpendicular direction regarding to moving axis, i.e., the tilted angle of V-beam. Please refer θ from Fig. 2a. The V-beam length, width, and temperature are kept as constants in calculation with respect to the Eq. (7). When we set up a target displacement of V-beam actuator regarding to tilted-mirror position for a particular attenuation value, the maximum force output of a single V-beam actuator is derived from Eq. (5) by considering overall relationships of equations (2–7). Basically, the V-beam actuators with smaller beam width and the longer beam length will provide larger corresponded values of maximum force output. For example, a V-beam actuator with beam length of $3,200\ \mu\text{m}$, beam width of $6\ \mu\text{m}$, beam thickness of $85\ \mu\text{m}$ and tilted angle of 0.6° will generate output force

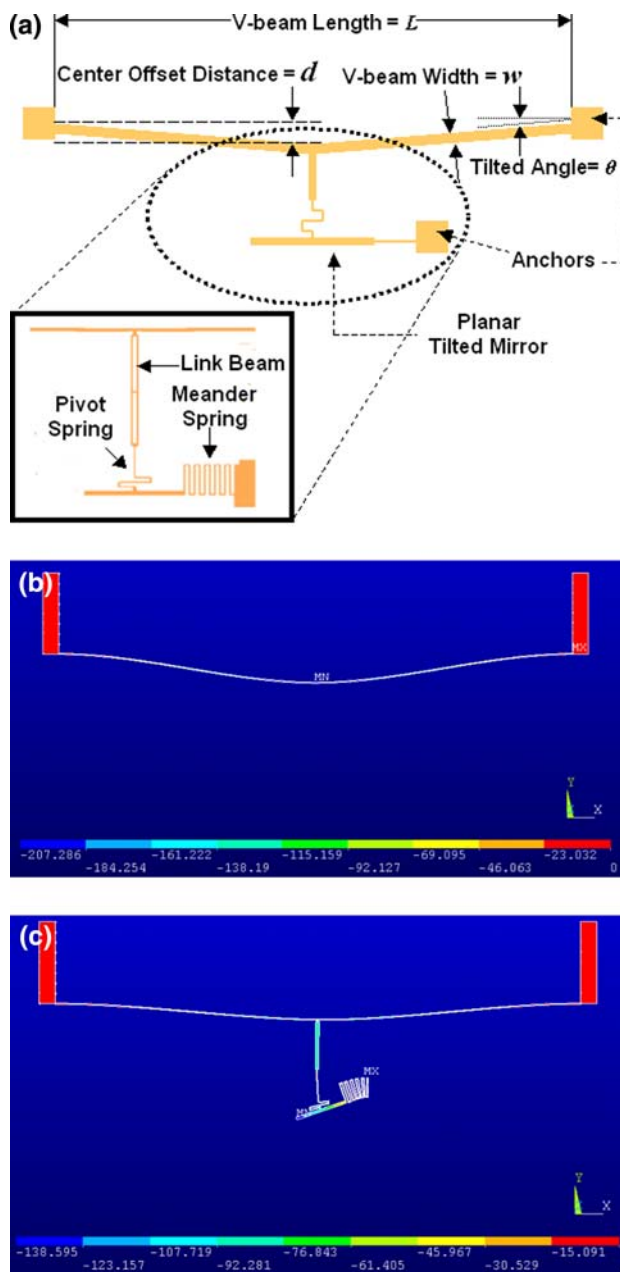


Fig. 2 **a** The top view of VOA device layout to show the denotation of geometrical parameters; **b** FEM simulated results of V-beam actuator; **c** FEM simulated results of proposed micromechanism for a VOA device

of about $3,750 \mu\text{N}$ with respect to $40 \mu\text{m}$ displacement. Moreover, we may consider the connected mirror plate with meander spring as case of V-beam actuator with loading toward opposite direction of moving direction. By separately calculating the displacement of mirror plate versus a force load on center of mirror plate, we may match such displacements under various geometrical combination of parameters of said meander spring according to the required design input from optical consideration, where this force is as same as the force

Table 1 Parameters used in analytical modeling of V-beam actuator force output

Parameter		Value
C	Experimental correlation factor	1.5
E	Young's modulus, silicon	169 GPa
g	Gap between beam and substrate	$2 \mu\text{m}$
h	Beam thickness	$85 \mu\text{m}$
k_a	Thermal conductivity, air	0.026 W/m-K
k_s	Thermal conductivity, silicon	150 W/m-K
P	Density, silicon	2330 kg/m^3
α	Thermal expansion coefficient, silicon	$2.51 \times 10^{-6} \text{ K}^{-1}$
ρ	Resistivity, silicon	$0.038 \Omega\text{-cm}$

generated by the V-beam actuator. On the other hand, we may simply conduct the finite element modeling (FEM) simulation. Fig. 2b shows the FEM results for a V-beam actuator with beam width of $6 \mu\text{m}$, beam thickness of $85 \mu\text{m}$ and beam length L of $3,200 \mu\text{m}$ by using ANSYS. The simulated maximum displacement caused by beam deformation of thermal expansion under 3 dc V is about $200 \mu\text{m}$. In the case of considering the VOA structure as shown in Fig. 2a, c, the simulated maximum displacement caused by beam deformation of thermal expansion under 3 dc V turns out to be $80 \mu\text{m}$, where the geometrical parameters of link beam, pivot spring and meander spring are quoted as: a link beam of $500 \mu\text{m}$ in length and of $10 \mu\text{m}$ in width and it including a compliant portion of $150 \mu\text{m}$ in length and of $5 \mu\text{m}$ in width; a pivot spring with the total length of $200 \mu\text{m}$ and the beam width of $5 \mu\text{m}$; a fivefold meander spring with the total length of $1,000 \mu\text{m}$ and the beam width of $5 \mu\text{m}$. These simulated data can provide the necessary information to us for determination of an optimized geometrical micromechanism structure for VOA devices.

3 Experimental results and discussions

The schematic drawing of the concept of said micromechanism can be realized in a planar structure as shown in Fig. 1c. The vertical reflective mirror, denoted as a planar tilted mirror and the meander spring, are micromachined from the device layer of a silicon-on-insulator (SOI) wafer, by using deep reactive ion etching (DRIE) process. After removing the underneath thermal oxides by wet etching, the planar tilted mirror and meander spring become the moving part. As shown in Fig. 3a, b, this tilted mirror is held by a meander spring at one end and is connected with an electrothermal actuator via a link beam with a folded spring. Two ends of the V-beam electrothermal actuator are also anchored onto the substrate, while the

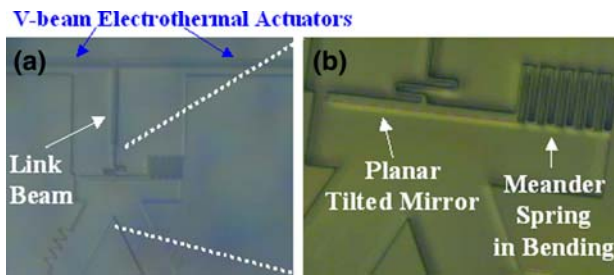


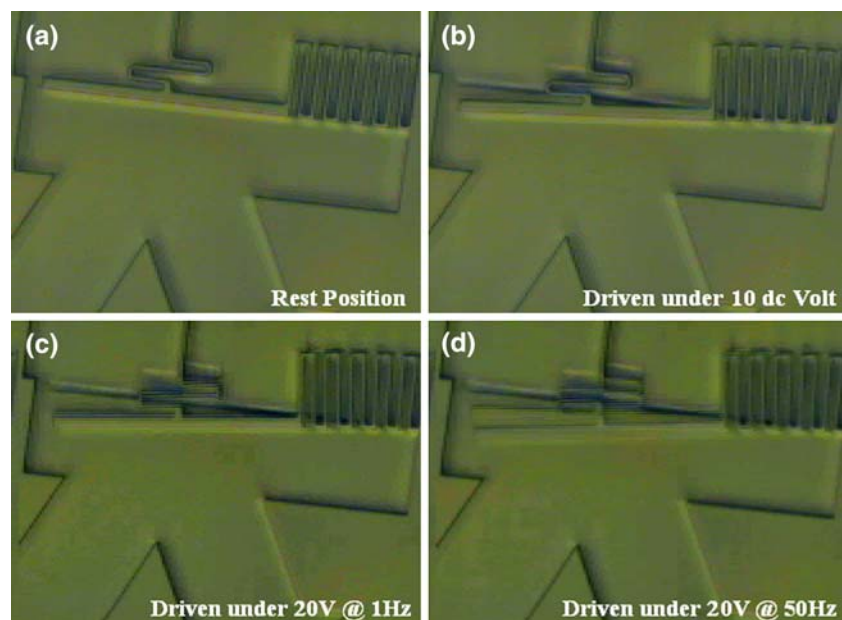
Fig. 3 VOA device comprises a planar tilted mirror driven by an electrothermal actuator. **a** CCD image of the tilted mirror, spring, link beam and electrothermal actuator of VOA device; **b** CCD image of the closed-up view of the tilted mirror, spring and trenches for accommodating fibers

other end of meander spring is fixed on the substrate as well. Thus, this micromechanism is anchored on substrate at three points. The high aspect ratio of beam cross-section of this structure gives high stiffness along with Z direction (perpendicular direction to substrate). The beam width, height, and length of one side of V-beam actuator is 6, 85 and 1,600 μm , respectively. The so-called tilted angle of V-beam is chosen to be 0.6° . The meander spring consists of fivefold meander structure with beam width of 5 μm and overall length of 1,000 μm , respectively. The spacing between two beams of the fivefold meander structure is 10 μm . The simulated maximum displacement regarding to this actuator is about 80 μm with respect to 16° tilted angle of mirror under a 3 dc V load. Briefly speaking, the simple and solid-supported structure with relatively smaller mass contributes on higher mechanical resonance frequency and mechanical strength in directions other than the moving direction. This novel design

offers mechanical prominence than previous reported designs.

In operation of device for bright type operation, two lens fibers are placed in the two trenches and faced toward the tilted mirror. The 1,550 nm laser is provided to device and the insertion loss is measured to be less than 0.8 dB typically, while we move and rotate these two fibers in order to reach the minimum value of the insertion loss. Then we apply electrical dc bias to the electrothermal actuator, the net volume expansion of actuator body caused by joule heating will turn to be a static displacement. This static displacement will provide the tilted mirror a displacement comprising rotational and translational displacement. Additionally, the continuous motion capability and flatness of mirror are crucial to the performance of VOA. Since, the attenuation versus the driving voltage should be a continuous curve. If the dynamic characteristics and the stability of mirror driven by electrothermal actuators at any transient points of a continuous actuated trace are not good enough, then the unwanted mirror distortion and deflection may cause deteriorated data of polarization dependent loss (PDL); or the repeatability of attenuation value versus a particular driving condition may vary from time to time. Fig. 4a presents the rest state of tilted mirror, while Fig. 4b shows the CCD image that was captured for tilted mirror regarding to 10 dc V. The same device was also tested at the 20 dc V, and the relative tilt angle is derived as 6.7° . Fig. 4c, d shows the captured CCD images of the transient state during vibration cycles under driving conditions of 20 V of 1 Hz and 20 V of 50 Hz, respectively. Based on the observation for static

Fig. 4 **a** CCD image of the tilted mirror VOA device staying at its initial state (zero attenuation); **b** CCD image of the tilted mirror VOA device at driving voltage of 10 dc V; **c** CCD image of the tilted mirror VOA device at driving voltage of 20 V and 1 Hz; **d** CCD image of the tilted mirror VOA device at driving voltage of 20 V and 50 Hz



deflection and transient state of dynamic vibration, we did not find distortion of spring and mirror in particular shapes. Only slight bending can be observed for meander-shaped spring, while the mirror plate is maintained as a straight shape.

In the practical application of VOA, a kind of VOA can block 100% incoming light signals at its initial state and permit a certain percentage of light to transmit toward output. This kind of VOA is called as the dark type of VOA. Its counterpart is the bright type of VOA that 100% incoming light signals are transmitting to output port at its initial state. We demonstrate the way of making dark type VOA based on current tilted mirror solution in present study too. First of all, Fig. 5a, b is the CCD images of bright type VOA at

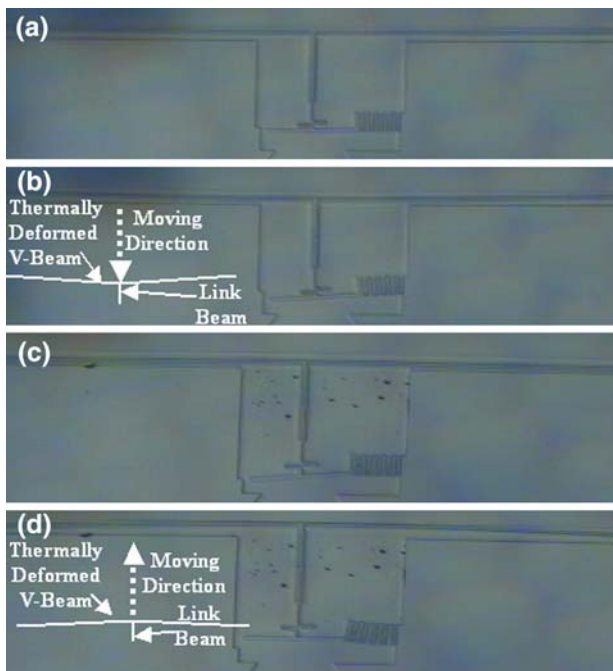


Fig. 5 **a** CCD image of initial state of bright type VOA driven by a forward moving V-beam actuator; **b** CCD image of actuated state of bright type VOA driven by a forward moving V-beam actuator; **c** CCD image of initial state of dark type VOA driven by a backward moving V-beam actuator; **d** CCD image of actuated state of dark type VOA driven by a backward moving V-beam actuator

initial and actuated states. A forward moving V-beam electrothermal actuator pushes the mirror to a tilted position, where the meander spring shows a gradient bended shape in Fig. 5b. In the beginning, the attenuation is kept at its zero state, i.e., the minimum insertion loss state. Comparing the Fig. 5a, b, we may figure out the obvious displacement provided by V-beam actuator and prominent tilted angle of mirror between the initial and actuated states. We measured the attenuation characteristics for both sorts of VOA devices. As shown in Table 2, the new tilted mirror type devices could be driven at the dc voltages of 5.5, 6.8, and 7.5 V pertinent to the attenuation of 10, 20, and 30 dB. Since we require only 7–8 V to drive the tilted mirror, and the driving voltage of 20 V used in experiments related to Fig. 4c, d is much larger than the voltage needed for VOA operation. Again, within the 20 V driving range, we did not find any evidence of unwanted mirror deformation. Therefore, the test of driving voltage higher than 20 V seems to be unnecessary.

Secondly, a backward moving V-beam electrothermal actuator is linked to a tilted mirror in the device rest state, as shown in Fig. 5c. Obviously this tilted position of mirror will lead the reflected light could not be coupled into the output port, i.e., the initial state of dark type operation, where the meander spring maintains at its original shape without deformation. When the dc voltage is applied to V-beam actuator, the tilted mirror will be pulled back from its initial tilted position, the reflected light starts to be coupled into output port gradually. Table 1 presents that, the voltages for 30, 20, 10 and 0 dB are 3.9, 4.6, 6.1 and 7.6–9.0 V, respectively. It is observed that the tilted mirror moved to a position without tilt, as shown in Fig. 5d. When the applied voltage is increased, the attenuation value is reduced regarding to the diminution of tilted angle, as shown in Fig. 5d. The 0 dB attenuation can be reached, if we adjust the fibers to appropriate positions when the mirror is maintained in such a position region.

It is found that the PDL of less than 0.1 dB for VOA devices using a tilted mirror within the 30 dB attenuation range. It is a quite interesting result. It points out the designs using single reflection mirror will derive

Table 2 Measured driving voltage, PDL and return loss at different attenuation states

Attenuation	Bright operation (dB)				Dark operation (dB)			
	0	10	20	30	0	10	20	30
Driving voltage (V)	0	5.5	6.8	7.5	7.6–9.0	6.1	4.6	3.9
Measured PDL (dB)	0.02	0.02	0.04	0.06	0.02	0.02	0.03	0.09
Measured return loss (dB)	52	51	50	49	51	50	49	50

much better PDL characteristics than the ones based on two reflection mirrors, e.g., retro-reflection type (Chen et al. 2004; Lee 2006b). The rather low PDL for single reflection mirror type of devices has been reported by Bashir et al. (2004) based on an electrostatic comb drive actuated reflective mirror, where the PDL is reported to be less than 0.1 dB for attenuation of less than 30 dB. The return loss is measured as small as 49 ~ 52 dB within 30 dB attenuation range.

4 Concluding remarks

A new type of electrothermally driven MEMS VOA device, tilted mirror VOA is proposed and characterized in this paper. Due to its feature of single-reflection light path, the tilted mirror VOA shows rather low PDL. In case, we make the spring of tilted mirror VOAs softer than present design, the driving voltage could be drastically reduced in the region of high attenuation range (e.g., 20–30 dB). Since both rotational and translational effect contributes on the mirror deflection pertinent to the tilted mirror type. Such contribution will be more obvious in high attenuation states. For example, softer spring could be realized by using more folds or longer beam of the meander-shaped spring.

The repeatability and stability of the static and transient characteristics of devices at room temperature ambient environment are rather promising. It points out the bright future regarding to the commercial applications. The current results also prove that electrothermal actuators should be a good alternative for driving MEMS VOAs.

Acknowledgments This work was supported in part by the grants from joint-funded research project based on Faculty Research Fund: R-263-000-358-112/133 of National University of Singapore and from Institute of Microelectronics of A*STAR, Singapore.

References

- Barber B, Giles CR, Askyuk V, Ruel P, Stulz L, Bishop D (1998) A fiber connectorized MEMS variable optical attenuator. *IEEE Photon Technol Lett* 10:1262–1264
- Bashir A, Katila P, Ogier N, Saadany B, Khalil DA (2004) A MEMS based VOA with very low PDL. *IEEE Photon Technol Lett* 16:1047–1049
- Cai H, Zhang XM, Lu C, Liu AQ, Khoo EH (2005) Linear MEMS variable optical attenuator using reflective elliptical mirror. *IEEE Photon Technol Lett* 17:402–404
- Chen C, Lee C, Lai Y-J, Chen W-C (2003a) Development and application of lateral comb drive actuator. *Jpn J Appl Phys* 42(6B):4067–4073
- Chen C, Lee C, Lai Y-J (2003b) Novel VOA using in-plane reflective micromirror and off-axis light attenuation. *IEEE Commun Mag* 41(8):S16–S20
- Chen C, Lee C, Yeh JA (2004) Retro-reflection type MOEMS VOA. *IEEE Photon Technol Lett* 16:2290–2292
- Chiou JC, Lin WT (2004) Variable optical attenuator using a thermal actuator array with dual shutters. *Opt Commun* 237:341–350
- Cochran KR, Fan L, DeVoe DL (2003) High-power optical micro switch fabricated by deep reactive ion etching (DRIE). *Proc. SPIE, MOEMS and miniaturized systems III*, Vol. 4983: 75–86
- Costello BJ, Jones PT, Lee H-S (2003) Optical switch. US Patent 6628856
- DeVoe DL (2002) Thermal issues in MEMS and microscale systems. *IEEE Trans Components Packaging Technol* 25(4):576–583
- Ford JE, Walker JA (1998) Dynamic spectral power equalization using micro-opto mechanics. *IEEE Photon. Technol Lett* 10: 1440–1442
- Gianchandani YB, Najafi K (1996) Bent-beam strain sensors. *J MEMS* 5(1):52–58
- Huang QA, Lee KS (1999) Analysis and design of a polysilicon thermal flexure actuator. *J Micromech Microeng* 9:64–70
- Isamoto K, Kato K, Morosawa K, Chong H, Fujita H, Toshiyoshi H (2004) A 5-Voperated MEMS variable optical attenuator by SOI bulk micromachining. *IEEE J Sel Top Quantum Elect* 10:570–578
- Kim YY, Yun SS, Park CS, Lee J-H, Lee YG, Lee HK, Yoon SK, Kang JS (2004) Refractive variable optical attenuator fabricated by silicon deep reactive ion etching. *IEEE Photon Technol Lett* 16:485–487
- Lee C (2005a) Monolithic-integrated 8CH MEMS variable optical attenuators. *Sens and Actuators A* 123–124:596–601
- Lee C (2005b) Arrayed variable optical attenuator using retro-reflective MEMS mirrors. *IEEE Photon Technol Lett* 17:2640–2642
- Lee C (2006a) Novel H-beam electrothermal actuators with capability of generating bi-directional static displacement. *Microsyst Technol* 12:717–722
- Lee C (2006b) MOEMS variable optical attenuator with improved dynamic characteristics based on robust design. *IEEE Photon Technol Lett* 18:773–775
- Lee KC, Lee SS (2004) Deep X-ray mask with integrated electrothermal micro XY-stage for 3D fabrication. *Sens Actuators A* 111:37–43
- Lee C, Wu C-Y (2005) Characterization of bi-stable micromechanism based on buckle spring and electrothermal V-beam actuators. *J Micromech Microeng* 15:11–19
- Lee C, Yeh JA (2005) Development of X-beam electrothermal actuators. *Microsyst Technol* 11:550–555
- Lee C, Lin Y-S, Lai Y-J, Tasi MH, Chen C, Wu C-Y (2004) 3-V driven pop-up micromirror for reflecting light toward out-of-plane direction for VOA applications. *IEEE Photon Technol Lett* 16:1044–1046
- Liu AQ, Zhang XM, Lu C, Wang F, Lu C, Liu ZS (2003) Optical and mechanical models for a variable optical attenuator using a micromirror drawbridge. *J Micromech Microeng* 13:400–411
- Maloney JM, Schreiber DS, DeVoe DL (2004) Large-force electrothermal linear micromotors. *J. Micromech Microeng* 14:226–234
- Marxer C, Griss P, de Rooij NF (1999) A variable optical attenuator based on silicon micromechanics. *IEEE Photon Technol Lett* 11:233–235

- Pan CS, Hsu W (1997) An electro-thermally and laterally driven polysilicon microactuator. *J Micromech Microeng* 7:7–13
- Que L, Park JS, Gianchandani YB (2001) Bent-beam electro-thermal actuators-part I: single beam and cascaded devices. *J Microelectromech Syst* 10:247–254
- Robinson KC (2000) Variable optical attenuator. US Patent 6137941
- Syms RRA, Zou H, Stagg J, Veladi H (2004) Sliding-blade MEMS iris and variable optical attenuator. *J Micromech Microeng* 14:1700–1710